Green stabilization of microscale iron particles using guar gum: bulk rheology, sedimentation rate and enzymatic degradation

Green stabilization of microscale iron particles using guar gum: bulk rheology, sedimentation rate and enzymatic degradation

Published in

Journal of Colloid And Interface Science

421 (2014) 33–43

Francesca Gastone[a], Tiziana Tosco[a], Rajandrea Sethi[a]*

[a] DIATI – Dipartimento di Ingegneria dell'Ambiente, del Territorio e delle Infrastrutture – Politecnico di Torino, C.so Duca degli Abruzzi 24, 10129 Torino, Italy
E mail addresses: francesca.gastone@polito.it, tiziana.tosco@polito.it, rajandrea.sethi@polito.it

* Corresponding Author:
Address: DIATI – Politecnico di Torino, C.so Duca degli Abruzzi 24, 10129 Torino, Italy
phone +39 (011) 564 7735; fax +39 (011) 564 7699 e-mail: rajandrea.sethi@polito.it

Abstract:

Guar gum can be used to effectively improve stability and mobility of microscale zerovalent iron particles (MZVI) used in groundwater remediation. Guar gum is a food-grade, environment friendly natural polysaccharide, which is often used as thickening agent in a broad range of food, pharmaceutical and industrial applications. Guar gum solutions are non-Newtonian, shear thinning fluids, characterized by high viscosity in static conditions and low viscosity in dynamic conditions. In particular, the high zero shear viscosity guarantees the MZVI dispersion stability, reducing the sedimentation rate of the particles thus enabling its storage and field operations.

In this work, a comprehensive rheological characterization of guar gum-based slurries of MZVI particles is provided. First, we derived a model to link the bulk shear viscosity to the concentration of guar gum and then we applied it for the derivation of a modified Stokes law for the prediction of the sedimentation rate of the iron particles. The influence of the preparation procedure (cold or hot dissolution and high shear processing) on the viscosity and on the stability of the suspensions was then assessed. Finally, the dosage and concentration of enzymes - an environment friendly breaker - were studied for enhancing and controlling the degradation kinetics of the suspensions. The derived empirical relationships can be used for the implementation of an iron slurry flow and transport model and for the design of full scale injection interventions.

Keywords:

Guar gum; microscale zero-valent iron; colloidal stability; shear thinning fluids; guar gum dissolution; guar gum bulk rheology; guar gum enzymatic degradation; sedimentation tests

Graphycal abstract:

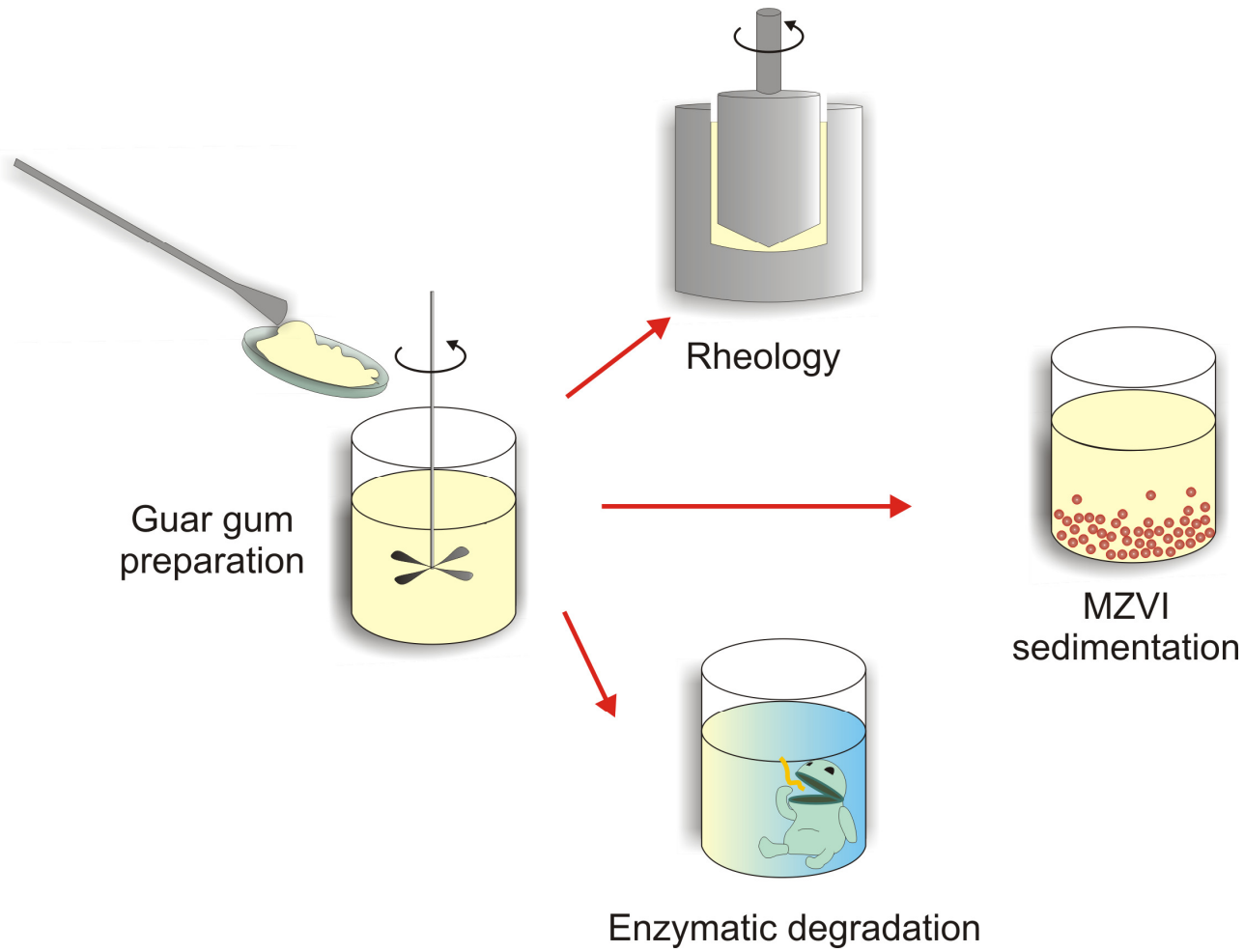

1. Introduction

Nanoscale zerovalent iron particles (NZVI) have been studied since several years for groundwater remediation in both laboratory and field-scale applications [1-6]. NZVI is injected into the subsurface dispersed in water-based slurries, applying iron concentrations in the order of tens of g/l [7]. More recently, also microscale iron particles (MZVI) were considered as an alternative to NZVI [8-10]. Both MZVI and NZVI were shown effective in degrading a wide range of contaminants. NZVI degradation kinetics are, as a general rule, faster, due to the higher specific surface area [11]. However, NZVI lifetime is shorter, compared to MZVI, with high consumption due to undesired side reactions in groundwater [10-11]. Handling of MZVI is easier and safer in field applications, being dry microscale particles chemically stable in air, while most of NZVI commercial products are available in aqueous suspensions or in modified atmosphere, to prevent combustion and explosion. Moreover, MZVI has a lower commercial cost and lower potential toxicity for the ecosystems [12]. Laboratory and field studies on MZVI reactivity and mobility have been recently addressed [8, 10, 13-14], even if a comprehensive study on an optimized preparation of MZVI suspensions and their characterization is still lacking. This work is aimed at filling this gap.

Both NZVI and MZVI are unstable when dispersed in pure water [2, 15-16]. The colloidal instability of the suspensions has a severe impact on preparation and storage of the iron slurries before injection, on the mobility of the particles in the porous medium, and consequently on the final radius of influence of field injections [17]. The aggregation and subsequent sedimentation of NZVI particles, due to strong magnetic particle-particle interactions [15], is successfully prevented by modifying the surface properties of the particles, using polymeric coatings [2, 18-19] or partial coating with other metals [18, 20-21]. On the other hand, the colloidal instability of MZVI is related to its larger size, which results in fast sedimentation [8, 10]. A modification of the dispersant fluid, rather than of the surface properties of the particles, is consequently needed. To meet this requirement, viscous polymeric solutions were studied, focusing on water-soluble, environment friendly compounds which can be safely released in the subsurface. In particular, starch, xanthan gum, cellulose, guar gum or mixtures of guar and xanthan viscoelastic gels were found successful in this sense in laboratory studies [8, 13, 22]. Such biological hydrocolloids, dissolved in water at concentrations in the order of few g/l, exhibit peculiar non-Newtonian, shear thinning properties,

which guarantee high viscosity in static conditions (thus hindering sedimentation during preparation and storage of the slurries), and low viscosity in dynamic conditions (thus limiting the pressure build up during injection).

Guar gum is selected in the present study as a stabilizing agent due to its easy degradation in the presence of specific enzymes and microorganisms, while other polymers, even more effective from the point of view of colloidal stability (eg. xanthan gum) are less suitable, as they are hardly degraded in subsurface conditions. Apart from degradation, guar gum solutions are stable over time, not prone to coagulation over a wide range of salinity and pH, which includes the typical conditions of environmental applications [23-24]. Guar gum is a food-grade polysaccharide extracted from seeds of the leguminous plant Cyamopsis tetragonolobus, commonly used as a thickening and stabilizing agent in a wide range of industrial applications (medicine, food, cosmetic), in enhanced oil recovery [25-26] and in situ remediation for the realization of permeable reactive barriers [27]. Guar gum is commercially provided as a water-soluble dry powder, which hydrates when dissolved in water forming a stable shear thinning solution with thixotropic properties. The hydration process however is not instantaneous, and spans several minutes to few hours. The kinetics depends on a number of factors, including molecular weight, final polymer concentration, temperature, and dry particle size [28]. Moreover, it was observed that, for guar gum as well as for most biopolymers, the complete hydration is never reached, and residual undissolved particles remain in suspension, along with aggregates of poorly hydrated molecules, called microgels [29-30]. Dissolution in warm water helps reducing the presence of both undissolved particles and microgels. Also post-filtration of the polymeric solutions is sometimes applied [29, 31].

Even if the polymeric solutions are extremely effective in improving the MZVI colloidal stability, the presence of polymeric chains adsorbed on iron particles limits the accessibility of the iron surface to dissolved contaminants, having a negative impact on MZVI reactivity. The process was shown to be reversible for guar gum in batch tests and at the field scale, thanks to the use of enzyme breakers, and reactivity was completely recovered after breakage and removal of polymeric chains [10, 27]. For these reasons, a complete removal of the polymer is desired after the injection in the subsurface.

This work presents a comprehensive study on the use of guar gum solutions as stabilizing agents to enhance the MZVI mobility in porous media, addressing the issues associated to the design of the MZVI/guar gum slurries, their colloidal stability and its impact on the injectability of the iron slurries. First, the optimal method for guar gum dissolution, with the aim of maximizing dissolution and therefore viscosity, is investigated. The presence of residual undissolved particles of guar gum

and microgels negatively affects the flow of guar gum solutions (and MZVI slurries) when injected in porous media. Solid particles are filtered in the pores, with a progressive reduction of porosity and permeability (clogging), and consequently an excessive, undesired pressure build up increasing over time during injection. A protocol is here defined for the optimized preparation of guar gum-based dispersions of MZVI in laboratory conditions, which can be up-scaled for field application. Then, a rheological characterization of guar gum solutions is provided for polymer concentrations in the range of field applications (1.5 to 7 g/l). The efficacy of the guar gum solutions in stabilizing MZVI particles of different size (1 to 30 μm) was tested in static sedimentation tests. Simple relationships were derived from rheological properties and sedimentation tests to link guar gum concentration, size of iron particles and desired stability time. They can be applied to estimate the guar gum concentration suitable for stabilizing the selected MZVI particles for the target time, which must be at least equal to the time required for the injection and for the spreading of the slurry in the subsurface. Finally, the enzymatic breakdown of guar gum is investigated using viscosity measurements for several enzyme concentrations, and a relationship is proposed for the tuning of the kinetics of the degradation process by controlling the enzyme concentration.

2. Background

2.1. Guar gum rheology

Guar gum solutions in the order of few g/l, corresponding to the concentration range required to improve the colloidal stability of MZVI slurries, are semi-diluted solutions characterized by a rheological shear thinning behavior. A semi-dilute solution is defined as a solution where the density of polymer chains is high enough to allow polymer-polymer interaction, giving rise to an entangled network. The concentration which ensures this interpenetrations is called overlap concentration c*: for a polymer concentration higher than the c*, the solution behaves as a shear thinning fluid, while for concentrations below c* (dilute regime) the rheological behavior is Newtonian. For guar gum solutions c* is typically in the range 1.3-1.4 g/l [32-33].

Semi-dilute solutions of guar gum exhibit a power law decrease of viscosity at intermediate shear rates, and two Newtonian plateaux at low and high shear rates. This behavior can be modeled with Cross, Carreau or similar formulations [34-36]. In this work, the Cross model is adopted:

$$\mu(\dot{\gamma}) = \mu_{\infty} + \frac{\mu_0 - \mu_{\infty}}{1 + (\lambda\dot{\gamma})^{\chi}} \qquad (1)$$

where μ is the fluid viscosity [M L^{-1} T^{-1}] at a given shear rate $\dot{\gamma}$ [T^{-1}], μ_0 is the Newtonian viscosity at low shear rate, μ_{∞} is the Newtonian viscosity at high shear rate, λ is the time constant, i.e. the reciprocal of the shear rate which separates the first Newtonian plateau from the power-law region [T], and χ is the model exponent [-].

A number of studies is reported in the literature linking the zero-shear viscosity μ_0 to concentration and molecular weight of dissolved biopolymers [37-40]. A commonly accepted law predicts a power-law dependence of specific viscosity μ_{sp} on polymer concentration:

$$\mu_{sp} = {c_{GG}}^{E} \qquad (2)$$

where c_{GG} is the dissolved guar gum concentration (or, more in general, the polymer concentration) [M L^{-3}], E is a number in the typical range 3-5 for semi-dilute solutions, 1-1.5 in the dilute regime [37, 41], and μ_{sp} is the specific (zero-shear) viscosity, defined as

$$\mu_{sp} = \frac{\mu_0 - \mu_{solv}}{\mu_{solv}} \tag{3}$$

where μ_{solv} is the viscosity of the solvent (in this case, water). Substituting (3) in (4) the correlation becomes

$$\mu_0 = \mu_{solv}\left(1 + {c_{GG}}^{E}\right) \tag{4}$$

Relationships for the dependence of the other Cross parameters on polymer concentration are almost lacking, with few exceptions [38, 42]. In particular, a power law dependence was proposed for the time constant λ [38, 43]:

$$\lambda = {c_{GG}}^{B} \tag{5}$$

where B is an exponent suggested to be equal to 3/2 for polyelectrolytes [43].
In this work, models (4) and (5) are adopted, and the values of E and B are inverse-fitted on experimental data. Similarly, a correlation is proposed for the dependence of the high-shear viscosity μ_∞ on the guar gum concentration, which is, to the authors' knowledge, lacking in the literature.

2.2. Sedimentation of microparticles in shear thinning polymeric solutions

The settling velocity v_s of a single particle suspended in a Newtonian fluid (e.g. microscale zero valent iron in water) is known to follow the Stokes law:

$$v_s = \frac{1}{18}\frac{\left(\rho_p - \rho_f\right)\cdot g \cdot d^2}{\mu} \tag{6}$$

where ρ_p and ρ_f are, respectively, the density of the particle and of the fluid [M L^{-3}], g is the modulus of gravity acceleration [L T^{-2}], and d is the particle diameter [L].

For non-Newtonian fluids, the viscosity (and consequently the sedimentation rate) depends on the shear rate experienced by the fluid close to the particle. The shear rate related to a sphere sedimenting at a velocity v_s can be estimated as [44]

$$\dot{\gamma} = 2\frac{v_s}{d_{Stokes}} \tag{7}$$

where d_{Stokes} is the sphere diameter. If the particle is not a sphere, d_{Stokes} represents the diameter of the sphere with same volume and density of the particle, which sediments at the same velocity. For distributions or aggregates of particles, d_{Stokes} is equal to $d_{50,Stokes}$, which represents, respectively, the average sphere diameter, or the average diameter of the spheres having the same mass and density of the aggregate (details hereinafter).

Several corrections to Stokes law have been proposed for non-Newtonian fluids, taking into account the shear-dependent viscosity [45-46]. Among these, for shear thinning fluids, Machač [47] proposed the use of the zero shear viscosity in (6), corrected by the drag coefficient correction function, which incorporates the non-Newtonian behavior of the fluid.

The prediction of sedimentation rates is, however, more challenging when dealing with concentrated suspensions [48]. The theories based on Stokes law or modified Stokes laws correctly predict the sedimentation rate of single particles and non concentrated suspensions, but are often inaccurate for concentrated ones, where particle interactions may become predominant. Contrary to Newtonian fluids, increasing particle concentration results in a faster sedimentation [49-51], with formation of typical vertical stratifications of inhomogeneous particle concentration [50]. This phenomenon, referred to as chained sedimentation, is more pronounced for elastic and highly thixotropic fluids, and for more concentrated suspensions [48, 50, 52].

3. Materials and methods

3.1. Materials

Guar gum was provided as dry powder (RANTEC HV7000, Ranchester, United States) with medium-fine granulation (nominal maximum grain size equal to 75 μm). Optical microscope observation of the dry powder (Figure 1) revealed an elongated structure of the particles, with average particle size of 68.1±34.5 μm (transverse size) and 184.6±98.8 μm (longitudinal size).

An enzymatic polymer breaker (LEB-H provided by Rantec, US, as aqueous dispersion with nominal concentration of 0.8% w/w) was used for guar gum degradation tests. These enzymes are effective in a wide range of pH (from 4.5 up to a 10) and temperature (below 60°C).

Four samples of iron microsized particles (Table 1 and Figure 2) were used in sedimentation tests: HQ and MS200 from BASF (Germany), H4 and H19 from Höganäs (Sweden).

3.2. Guar gum dissolution

Several guar gum preparation procedures were tested:

- as received (AR): the guar gum was dissolved in MilliQ water at 20°C with continuous stirring for 30 min;
- thermally dissolved (T60): the guar gum powder was dissolved in MilliQ water at 60°C, with continuous stirring for 30 min,
- thermally dissolved and wet centrifuged (T60C): the thermally dissolved guar gum (T60) was centrifuged for 10 minutes at 4000 rpm after overnight hydration;
- thermally dissolved and filtered (T60F): the thermally dissolved guar gum (T60) was filtered through a porous medium after overnight hydration.

For all procedures, the guar gum solutions were prepared at a concentration of 6 g/l, degassed 5 mins using a vacuum pump to remove air bubbles, stored overnight at 4°C to ensure the complete hydration of the soluble fraction of the polymer powder [33], and diluted to the desired polymer concentration prior to use. The effectiveness of the procedures was tested for polymer concentrations of 3 g/l and 4 g/l in rheological measurements and sedimentation tests. A wider

range of concentrations (1.5 to 7 g/l) was considered for the rheological characterization of the suspensions.

Sodium azide was added as a preservative for all samples (except those used in enzyme degradation tests), to avoid possible bacterial degradation during storage.

3.3. Rheological characterization

Rheological measurements on guar gum solutions were performed at 20°C using an Anton Paar rheometer MCR 301 equipped with concentrical cylinders. The rheological tests performed include shear viscosity measurement and evaluation of the degradation kinetics in the presence of enzymes.

The shear viscosity was measured as a function of shear rate for different guar gum concentrations (1.5 g/l to 7 g/l) and preparation procedures, exploring a shear rate range from 10^{-2} to 10^{4} s^{-1} (ranges may differ of one order of magnitude depending on the test performed).

Storage, G', and loss, G'', moduli were measured as a function of the frequency at a given stress of 0.01 Pa (i.e. frequency sweep test) for all guar gum concentrations, exploring frequencies ranging from $6.28 \cdot 10^{-2}$ to $6.28 \cdot 10^{1}$ rad/s. The stress was chosen small enough to preserve the polymer structure, thus ensuring the measurement in the linear viscoelastic (LVE) regime, i.e. the range of frequencies within which both moduli are independent of frequency. This range was obtained with the so-called amplitude sweep measurement (data not reported).

3.4. Preparation of iron slurries

Iron slurries were prepared at a particle concentration of 20 g/l. The iron particles were first dispersed in water, sonicated for 5 mins to promote the breakage of aggregates, and then mixed with the hydrated guar gum solution using a high speed rotor-stator system (UltraTurrax) to break residual MZVI aggregates. The slurry was then degassed under vacuum while sonicated for 15 mins to remove the residual air. The dispersion procedure was described more in detailed by Xue and Sethi [13].

3.5. MZVI sedimentation tests

Sedimentation tests were performed to evaluate the colloidal stability of MZVI slurries for different guar gum concentrations and preparation procedures. The suspensions were placed in elongated cuvettes and the iron concentration was continuously monitored over time at a fixed height (average sedimentation path *L/2* of 0.015 m), using a susceptibility sensor (Bartington, UK) [8]. The data were analyzed in terms of sedimentation half time (t_{50}), namely the time when the detected concentration reaches half the initial value. The corresponding average sedimentation rate (v_s) was obtained as $(L/2)/t_{50}$.

For thermally dissolved guar gum (T60C), the influence of polymer concentration (in the range 1.5 to 7 g/l) and particle size (1.1 to 27 µm) was investigated in details. An iron concentration of 20 g/l was chosen as a typical value for field applications of MZVI.

The value of the average particle size $d_{50,Stokes}$ considered for sedimentation tests (Table 1) is not, as a rule, equal to the average diameter d_{50} measured with dynamic light scattering. Only for the spherical MS200 particles the two values coincide. For HQ particles, conversely, which are not completely disaggregated in the slurry (optical microscope images, not reported), the $d_{50,Stokes}$ was calculated as the equivalent diameter of the sphere with the same volume as the aggregate. For H4 (elongated particles) and H19 (highly irregular particles), the average volume of single particles was estimated from SEM images and used to calculate the average equivalent sphere diameter (Table 1).

3.6. Guar gum adsorption on microparticles

For the analysis of the experimental data of sedimentation tests, a correction to guar gum concentration of the dispersion was applied: when iron particles are dispersed in a polymeric solution, a fraction of the polymer adsorbs on the particle surface, thus resulting in an overall decrease of free polymer concentration and, consequently, of the fluid viscosity [13]. The mass of adsorbed polymer, directly proportional to the particle specific surface area (SSA), was estimated from viscosity measurements of guar gum solution before and after addition of the iron particles.

3.7. Enzymatic degradation tests

Rheological tests were performed to monitor the enzymatic degradation of guar gum solutions at a concentration of 3 g/l (T60C preparation procedure, no preservative added). Several mass ratios of

breaker to guar gum were considered, i.e. 1:1250, 1:6250, 1:12500, 1:125000, corresponding to a ratio of mass of commercial breaker solution to guar gum mass of 1:10, 1:50, 1:100; 1:1000, respectively (this latter notation will be used when discussing the results). The enzymes were added after the sample loading and briefly pre-mixed in the rheometer cup before the test (15 s at a shear rate of 100 s^{-1}) to guarantee a homogeneous distribution.

The dynamics of the enzymatic degradation process was monitored by rheological measurements. All studies reported in the literature are carried out through shear experiments, which apply large deformations to the sample [53-56]. However, if the shear is applied for a long time, the sample can undergo mechanical degradation, which cannot be easily separated from the enzymatic one. In this work an alternative measuring procedure is proposed, based both on shear and on oscillatory tests. Oscillatory tests were performed at the early stage of the degradation process, in order to avoid mechanical degradation due to the application of an extra-stress. When the viscosity reached at least 50% of its initial value (i.e. late degradation stage), the degradation process was monitored by means of shear viscosity, more suitable for lower viscosity values.

The initial undisturbed conditions were assessed by measuring both shear and complex viscosity at shear rates frequencies ranging from 0.5 s^{-1} and 50 s^{-1} before enzymes were added into the guar gum solution. Oscillation tests were performed in the Linear Visco-Elastic (LVE) range, corresponding to small deformations of the sample [57-60]. Therefore the complex viscosity, $|\eta^*(\omega)|$, was measured continuously over time at a constant stress (0.05 Pa) and variable frequency ω (1, 1.58, 5, 15.8 rad). According to the Cox-Merz rule [61], the shear viscosity at a small shear rate (lower than 20 s^{-1} for the studied solution) can be considered equal to the complex viscosity at the same angular frequency. Later on, shear viscosity was measured each 2 hours at the same shear rates.

4. Results and discussion

4.1. Optimization of guar gum preparation

Different procedures were tested for the preparation of guar gum solutions, with the aim of maximizing the dissolution of the guar gum powder, thus reducing the presence of undissolved residual particles and microgels, and maximizing viscosity. The efficacy of the procedures was assessed basing on three criteria: first, a qualitative evaluation of solid residuals was performed via optical microscope observation; second, the final solution viscosity was measured and compared; third, the efficacy in stabilizing MZVI suspensions was quantified.

Optical microscope images (Figure 3) show that dissolution at room temperature (procedure AR, Figure 3a) results in a high number of residual undissolved particles (bright continuous structures) associated to blobs of partly dissolved material, namely microgels (shadowed larger structures), which often have a solid nucleus. When guar gum is dissolved in warm water (procedure T60, Figure 3b), the number of solid particles is lower, and the dissolution is in general more efficient (compare the less evident and sharp contours of microgels). Further centrifugation of the guar gum solution (procedure T60C, Figure 3c) greatly reduces the number and size of solid particles. Occasional small microgels without solid nucleus are still present. The identification of an effective and easy procedure for the minimization of undissolved particles and microgels is particularly important for the application of guar gum solutions envisioned in this work: when guar gum solutions and guar gum based slurries of iron particles are injected in porous media, solid residuals are expected to be filtered in the soil, due to their large size. If their amount is high, they may have a negative impact on the porous medium permeability and porosity, giving rise to clogging and thus increasing pressure build up during the injection. This is a particularly undesired process, since it has a negative impact on both mobility and distribution of the iron particles. If the porous medium is clogged, the iron particles are retained close to the injection well and their migration length is very limited, so causing an extra pressure, with possible formation of preferential flow paths in the porous medium, and a consequent highly non homogeneous distribution of the iron particles at the end of the injection.

The impact of the preparation procedure on the fluid viscosity can be evaluated from the rheograms reported in Figure 4. It can be noticed that the low-shear viscosity for AR samples is the lowest one,

while at high shear rates the difference is less relevant. Also, for the T60C samples the viscosity is slightly lower compared to T60 samples, suggesting that centrifuging removes not only undissolved particles, but also a limited quantity of dissolved polymer.

The preparation procedures were then evaluated in sedimentation tests for HQ particles. The experimental results (Figure 5) indicate that the use of warm water (T60 and T60C) improves guar gum dissolution, thus resulting in slower sedimentation. Filtration (T60F) or centrifugation (T60C) provided very similar results, and the two procedures can be considered equivalent.

4.2. Rheology of guar gum solutions

The rheological properties of guar gum solutions prepared following the procedure T60C were studied in the range of polymer concentration 1.5 to 7 g/l. The shear viscosity was measured over the shear rate range 10^{-3}-10^{4} s^{-1}, corresponding to the range relevant to the application of guar gum for improving stability of MZVI suspensions: the low shear rate values are experienced in sedimentation tests, while shear rate in the order of few thousands s^{-1} are expected during the injection in the field close to the well.

The measured viscosity is reported in Figure 6 (point values), showing a typical shear thinning behavior, with increasing viscosity with increasing guar gum concentration. For each guar gum concentration, the experimental data were least-squares fitted against the Cross eq (1) (solid lines), showing a very good agreement between model and experimental data. The parameters μ_0, μ_∞, λ and χ were obtained independently for each curve (Figure 7).

As anticipated in the introduction, the aim of the rheological characterization is to derive a rheological model able to describe the dependence of viscosity on both shear rate and polymer concentration, thus providing a tool for the design of MZVI suspensions. To this purpose, the dependence of the Cross parameters on guar gum concentration was analyzed and modeled. For the zero-shear viscosity μ_0 eq. (4) was successfully applied (Figure 7a). For the characteristic time λ, a modified formulation of eq. (5) was applied (Figure 7b). The exponent χ was assumed constant with guar gum concentration (Figure 7c). Conversely, for the high-shear Newtonian viscosity μ_∞ an asymptotic increase from water viscosity μ_w up to an almost constant value (ultimate viscosity $\mu_{\infty,ult}$) can be identified. Because no relationship was found in the literature for the dependence of

μ_∞ on the polymer concentration, a correlation was derived, representing the observed trend (Figure 7a).

In summary, the complete rheology model is

$$\begin{cases} \mu(\dot{\gamma}, c_{GG}) = \mu_\infty(c_{GG}) + \dfrac{\mu_0(c_{GG}) - \mu_\infty(c_{GG})}{1 + \left[\lambda(c_{GG})\dot{\gamma}\right]^\chi} \\ \mu_0 = \mu_w\left(1 + c_{GG}^E\right) \\ \lambda = A c_{GG}^E \\ \mu_\infty(c_{GG}) = \mu_{\infty,ult} - \left(\mu_{\infty,ult} - \mu_w\right) e^{-c_{GG}} \end{cases} \quad (8)$$

where the fitted parameters are $\chi = 0.713$, $E = 4.59$ (in agreement with the typical range of exponents reported in the literature for semi-dilute polymeric suspensions), $A = 5.06 \cdot 10^{-4}$, $B = 4.04$, and $\mu_{\infty,ult} = 3.60 \cdot 10^{-3}$ Pa·s.

For $c_{GG} = 0$ the model (8) reduces to the solvent constant viscosity (μ_w).

The rheological curves calculated using the complete model (8) with the fitted coefficients are reported in Figure 6 (dashed lines), showing a good agreement with experimental data (point values) and Cross curves fitted independently (solid lines). The model eq. (8) is less accurate only for the lowest concentration, which is likely to be at the limit of the semi-dilute regime (i.e. transition between Newtonian and non-Newtonian behavior).

4.3. MZVI dispersion in guar gum: sedimentation tests

The efficacy of the guar gum solutions prepared following the procedure T60C was finally evaluated in terms of colloidal stability of MZVI colloidal suspensions.

The influence of iron particles on the viscosity of the dispersions was evaluated in rheological tests. Compared to guar gum solutions without particles, iron slurries exhibit a very limited reduction of viscosity at low and intermediate shear rates (Figure 8), which can be attributed to the adsorption of a fraction of free polymer chains to the iron particles surface [13]. The mass of absorbed guar gum per unit surface area of iron particles, m_{ads} [M/L^2], equal to $8.4 \cdot 10^{-3}$ g/m^2 was estimated from data previously reported [13]. The corresponding reduction in free polymer concentration was applied for each guar gum concentration and each particle, depending on particle SSA. For 20 g/l MZVI dispersions in guar gum, the correction is equal to 0.152 g/l, 0.030 g/l, 0.420 g/l, 0.016 g/l of guar

gum for HQ, MS200, H19 and H4 respectively. The correction can be neglected for particles with low SSA, while it is recommended in case of high SSA (eg. H19).

Figure 9 reports an example of sedimentation curves for H4 particles, presented as normalized particles concentration C/C_0 at a fixed position of the vertical cuvette, as a function of time. A qualitative observation of the curves indicates that increasing guar gum concentration results in a more stable solution. Furthermore, the sedimentation process can be divided into two stages: at first the suspension is almost stable, then an evident settling of the particles occurs, with a fast decay of concentration. The duration of first step (t_{st}, stability time) and of the second one (t_{sed}, sedimentation time) increase with increasing guar gum concentration, and are aligned along a straight line in a semi-log graph (Figure 9). This behavior, typical of shear thinning fluids with memory, is consistent with experimental observations of particles sedimenting in xanthan solutions, and is not observed in Newtonian fluids [50]. In our experimental data, the phenomenon is more pronounced at high guar gum concentrations, and less evident at the lowest ones. Since guar gum solutions exhibit a very limited memory effect, compared to xanthan gum and guar gum-xanthan gum mixtures [13], it is possible to assume that the memory effect can be in most cases neglected, and that the sedimentation process can be quantified referring to an average sedimentation rate v_s and average sedimentation half-time t_{50}.

The sedimentation half times and the corresponding sedimentation rates obtained from the laboratory tests for all particles (HQ, MS200, H19 and H4) dispersed in guar gum solutions in the range 1.5 to 7 g/l are reported in Figure 10 as point values. The Stokes law (6) can be applied for the estimate of sedimentation rates, provided that a modified value of viscosity is used, taking into account the (limited) reduction of the shear thinning viscosity of the fluid due to the shear rate exerted by the particle sedimenting through it. In this sense, the shear rate for the sedimenting particle can be calculated using eq. (7), and applied in the Cross model (8), which provides the corrected viscosity to be used in Stokes law (6). Therefore, the following set of equations was solved iteratively to calculate the sedimentation rate:

$$\begin{cases} v_s = \dfrac{1}{18}\dfrac{\left(\rho_p - \rho_f\right)\cdot g \cdot d_{50,Stokes}^2}{\mu\left(\dot{\gamma}\right)} \\ \dot{\gamma} = 2\dfrac{v_s}{d_{50,Stokes}} \\ \mu\left(\dot{\gamma}, c_{GG}\right) = \mu_\infty\left(c_{GG}\right) + \dfrac{\mu_0\left(c_{GG}\right) - \mu_\infty\left(c_{GG}\right)}{1 + \left[\lambda\left(c_{GG}\right)\dot{\gamma}\right]^\chi} \end{cases} \tag{9}$$

For all particles and guar gum concentrations, the estimated sedimentation shear rate, in the range 10^{-3} s^{-1} (small particles, high polymer concentration) to 10 s^{-1} (large particles, low polymer concentration), indicates that the sedimentation takes place in the low-shear Newtonian region, or close to it, with a limited impact of the non-Newtonian properties of the fluid. The prediction of experimental sedimentation rate obtained by the modified Stokes law (eq. 9) is extremely satisfactory (Figure 10). Minor discrepancies are found only for HQ particles, and can be attributed to the presence of small aggregates of approximately 3 to 15 particles, thus characterized by a range of sedimentation rates.

4.4. Enzymatic degradation

The enzymatic degradation process of the guar gum solution at 3 g/l was monitored for different enzymes concentrations (1:10, 1:50, 1:100, 1:1000) at early and late stages using, respectively, oscillation and rotational tests. Figure 11 shows the variation of viscosity as a function of the shear rate measured at different times for two enzymes concentrations. Figure 12a reports the degradation kinetics at the four enzymes concentrations for small shear rate (1 s^{-1}) i.e. on the first Newtonian plateau. The graph indicates that, after 3 hours, the viscosity of the solution containing the highest enzymes concentration (1:10) decreased more than one order of magnitude, while for the 1:1000 sample the decrease was only 50% of the initial value. A control measurement performed on guar gum samples without addition of enzymes (Figure 12) evidenced that in the absence of the breaker the viscosity is constant over time, suggesting that the guar gum solution is stable from a colloidal point of view.

Since degradation profiles at different enzymes concentrations are characterized by a similar shape, they can be superimposed by shifting them along time [55], thus obtaining the so-called master curve. Figure 12b reports the master curve as a function of the reduced time $h \cdot t$, where h is linearly dependent on enzymes concentration as $h=H \cdot (c_{enzymes}/c_{GG})$ being H the line slope, equal to 500. The shape of the master curve suggests that the degradation process can be divided in three regimes: an early and late time behaviour, where the degradation kinetics is slower, and an intermediate power law interval, where the breakdown rate is faster. The existence of the two plateuax indicates that both the initial zero shear viscosity and the final asymptotic viscosity value are the same for all the enzymes concentrations and depend only on the initial guar gum concentration.

The superposition of the curves at different enzymes concentrations leads to two main results: first, the possibility of extending the measuring range also where technical limitations arise (eg. at the early stages of degradation when the enzyme concentration is very high and thus the degradation process is fast). Second, an a-priory prediction of the enzymes concentration to be used in a field application can be retrieved directly from the master curve, without perforiming multiple degradation tests for several enzyme or guar gum concentrations. In field applications, enzymes are usually dosed into the slurry immediately prior to injection. As a consequence, once the field injection has been designed (namely iron particles size and concentration, polymer concentration, slurry volume, injection rate and consequently injection time), a propert enzyme concentration is to be selected, which can guarantee a guar gum degradation rate slow enough to still have a sufficiently viscous slurry until the end of the injection. In this sense, graphs like those reported in Figure 12 can be used.

5. Conclusions and implications for field injection

The work herein presented is the first part of a comprehensive study on the enhancement of colloidal stability and mobility in porous media of MZVI particles dispersed in guar gum solution. It is aimed at providing a complete characterization of guar gum solutions for improved stability of iron microparticles, and at identifying efficient procedures for the preparation of iron slurries, as well as relationships for the dimensioning of such suspensions for field applications.

The first target was the optimization of the guar gum dissolution procedure, both maximizing viscosity for a given polymer concentration, and minimizing the content of residual solid particles using laboratory procedures easy to be up-scaled to field applications. The comparative evaluation of several procedures evidenced that the use of warm water improves dissolution, and therefore the final solution viscosity. A post-treatment of the guar gum solution may be necessary if a further removal of undissolved residual particles is required. In this sense, both centrifuging and filtration are effective, with comparable removal efficiency. From a practical point of view, centrifugation is an easier approach at the laboratory scale, while in-line filtration through a porous bed may be more efficient in field-scale applications.

Guar gum solutions exhibit a pronounced shear thinning behavior, resulting in high viscosity at low shear rates, and low viscosity at high shear rates. Both conditions play a role in laboratory and field injection of MZVI slurries amended with guar gum: the first is representative of static conditions, when MZVI slurries are stored and handled before injection, the second corresponds to dynamic conditions, when the slurries are injected into the subsurface, experiencing high flow rates in pipes and in the porous medium. For this reason, a complete rheological characterization of guar gum solutions and MZVI slurries is crucial in the framework of this study. A modified Cross model was derived for guar gum viscosity as a function of shear rate and polymer concentration and can be used for the prediction of pressure build up arising from guar gum injection in porous media [62].

The colloidal stability of MZVI dispersed guar gum was also assessed for an iron concentration representative of field applications (20 g/l). The MZVI sedimentation rate was found dependent on particle size and guar gum concentration. Contrary to other polymers (eg xanthan gum - guar gum mixtures [13]), guar gum solutions do not provide an indefinitely stable suspension, due to the absence of yield stress. Conversely, even if the dispersant fluid is non-Newtonian, the sedimentation process can be correctly modeled by the Stokes law, provided that the shear rate dependent

viscosity is used. From a practical point of view, the estimate of the sedimentation rate is required for the optimization of MZVI dispersions for field application. When a specific MZVI particle have been selected for laboratory or field application, the guar gum concentration which can guarantee a stable suspension for the desired time is to be identified. For this purpose, eq. (9) can be used. However, a first estimate can also be obtained assuming that sedimentation takes place at a shear rate sufficiently low, so that guar gum viscosity can be approximated with the zero shear viscosity μ_0. This approximation is acceptable in most real applications. Under this hypothesis, the set of eq. (8-9) can be combined and the required guar gum concentration can be calculated as

$$c_{GG} = \left(\frac{1}{18} \frac{(\rho_p - \rho_f) \cdot g}{\mu_w} \frac{d_{50,Stokes}^2}{v_s} - 1 \right)^{1/E} \qquad (10)$$

where v_s is the maximum target sedimentation rate (estimated from the delivery and storage plant, for example based on the size of the storage tank or on the diameter of the pipes used in the injection).

Finally, in order to re-establish initial iron particles reactivity, it is necessary to remove the polymer by means of guar gum breakers. The degradation process of polymeric solutions can be successfully monitored along time at a laboratory scale using a mixed technique based both on dynamic oscillation (early stage) and shear (late stage) experiments. The tests performed pointed out that the degradation process strictly depends on the applied enzyme to guar gum mass ratio, and that the degradation rate can be tuned through the breaker dosage. This dependence can be modeled using a single degradation master curve, determined in the laboratory from few selected degradation tests. For field applications, once the polymer concentration and the injection time (and consequently the time for which the MZVI suspension has to be stable) have been defined, the use of the master curve would allow an a priory prediction of the correct enzymes concentration to be used to guarantee a sufficient viscosity to the polymeric suspension until it has been delivered into the subsurface. Finally, it is worth to mention that the use of enzymes to accelerate and control the degradation of guar gum was preferred to other methods since it can guarantee a full environmental compatibility, and the commercial breaker used here does not exhibit human nor environmental toxicity. Furthermore, for applications in aquifer systems with a potential for biodegradation of organic contaminants, the presence of degraded guar gum can result in a concurrent beneficial stimulation of the bacterial activity, which can represent an effective long-term degradation mechanism complementary to the short-term a-biotic degradation provided by microscale reactive particles.

Acknowledgement

The work was co-funded by the EU research project AQUAREHAB (FP7, Grant Agreement n. 226565).

References

[1] X.Q. Li, D.W. Elliott, W.X. Zhang, Critical Reviews in Solid State and Materials Sciences 31 (2006) 111.
[2] A. Tiraferri, K.L. Chen, R. Sethi, M. Elimelech, J Colloid Interf Sci 324 (2008) 71.
[3] P.G. Tratnyek, R.L. Johnson, Nano Today 1 (2006) 44.
[4] D. O'Carroll, B. Sleep, M. Krol, H. Boparai, C. Kocur, Advances in Water Resources 51 (2013) 104.
[5] R.L. Johnson, J.T. Nurmi, G.S. O'Brien Johnson, D. Fan, R.L. O'Brien Johnson, Z. Shi, A.J. Salter-Blanc, P.G. Tratnyek, G.V. Lowry, Environmental Science & Technology 47 (2013) 1573.
[6] M. Oostrom, T.W. Wietsma, M.A. Covert, V.R. Vermeul, Ground Water Monitoring & Remediation 27 (2007) 122.
[7] T. Tosco, M. Petrangeli Papini, C. Cruz Viggi, R. Sethi, Journal of Cleaner Production (2014) DOI: 10.1016/j.jclepro.2013.12.026.
[8] E. Dalla Vecchia, M. Luna, R. Sethi, Environmental Science & Technology 43 (2009) 8942.
[9] T. Tosco, R. Sethi, Environmental Science and Technology 44 (2010) 9062.
[10] M. Velimirovic, H. Chen, Q. Simons, L. Bastiaens, Journal of Contaminant Hydrology 142-143 (2012) 1.
[11] T. Almeelbi, A. Bezbaruah, J Nanopart Res 14 (2012).
[12] C. Lee, J.Y. Kim, W.I. Lee, K.L. Nelson, J. Yoon, D.L. Sedlak, Environmental Science & Technology 42 (2008) 4927.
[13] D. Xue, R. Sethi, J Nanopart Res 14 (2012).
[14] M. Velimirovic, M. Uyttebroek, L. Bastiaens, C. De Boer, N. Klaas, J. Braun, T. Tosco, M. Luna, F. Gastone, R. Sethi, H. Sapion, H. Eisenmann, P.-O. Larsson, in: VITO, (Ed.)^(Eds.)1st European Symposium on Remediation Technologies and their Integration in Water Management, Barcelona, 2012, p 113.
[15] E. Dalla Vecchia, M. Coisson, C. Appino, F. Vinai, R. Sethi, Journal of Nanoscience and Nanotechnology 9 (2009) 3210.
[16] T. Phenrat, H.-J. Kim, F. Fagerlund, T. Illangasekare, R.D. Tilton, G.V. Lowry, Environmental Science & Technology 43 (2009) 5079.
[17] C.M. Kocur, D.M. O'Carroll, B.E. Sleep, Journal of Contaminant Hydrology 145 (2013) 17.
[18] F. He, D. Zhao, Environmental Science and Technology 39 (2005) 3314.
[19] N. Saleh, K. Sirk, Y. Liu, T. Phenrat, B. Dufour, K. Matyjaszewski, R.D. Tilton, G.V. Lowry, Environmental Engineering Science 24 (2007) 45.
[20] D.W. Elliott, W.X. Zhang, Environmental Science and Technology 35 (2001) 4922.
[21] S.M. Hosseini, T. Tosco, Water Research 47 (2013) 326.
[22] M.J. Truex, V.R. Vermeul, D.P. Mendoza, B.G. Fritz, R.D. Mackley, M. Oostrom, T.W. Wietsma, T.W. Macbeth, Ground Water Monitoring and Remediation 31 (2011) 50.
[23] R.J. Chudzikowski, Journal of Cosmetic Science 22 (1971) 43.
[24] Q. Wang, P.R. Ellis, S.B. Ross-Murphy, Food Hydrocolloids 14 (2000) 129.
[25] C.G. Mothé, D.Z. Correia, F.P. De França, A.T. Riga, Journal of Thermal Analysis and Calorimetry 85 (2006) 31.
[26] R. Khachatoorian, I.G. Petrisor, C.C. Kwan, T.F. Yen, Journal of Petroleum Science and Engineering 38 (2003) 13.
[27] A. Di Molfetta, R. Sethi, Environmental Geology (2006).
[28] Q. Wang, P.R. Ellis, S.B. Ross-Murphy, Carbohydrate Polymers 74 (2008) 519.

[29] C. Chaudemanche, T. Budtova, Carbohydrate Polymers 72 (2008) 579.
[30] G. Chauveteau, N. Kohler, Society of Petroleum Engineers journal 24 (1984) 361.
[31] E. Treiber, Industrial & Engineering Chemistry Product Research and Development 20 (1981) 231.
[32] R.H.W. Wientjes. Rheology of Associative Biopolymers. University of Twente, 2001.
[33] Q. Wang, P.R. Ellis, S.B. Ross-Murphy, Carbohydrate Polymers 49 (2002) 131.
[34] M.M. Cross, Journal of Colloid Science 20 (1965) 417.
[35] M. Reiner, Deformation, strain, and flow; an elementary introduction to rheology. [2d ed., Interscience Publishers, New York,, 1960.
[36] P.J. Carreau, Trans Soc Rheol 16 (1972) 99.
[37] P.R. Ellis, W. Q, R. P., R. Y., R.-M.S. B., in: D.M.L. Cho S., (Ed.)^(Eds.)Handbook of dietary fibers; Marcel Dekker, Inc., New York, 2001, p 613.
[38] D. Risica, A. Barbetta, L. Vischetti, C. Cametti, M. Dentini, Polymer 51 (2010) 1972.
[39] Y. Heo, R.G. Larson, Journal of Rheology 49 (2005) 1117.
[40] B. Launay, G. Cuvelier, S. Martinez-Reyes, Carbohydrate Polymers 34 (1998) 385.
[41] G. Robinson, S.B. Ross-Murphy, E.R. Morris, Carbohydrate Research 107 (1982) 17.
[42] X. Lopez. Pore-Scale Modelling of Non-Newtonian Flow. Imperial College, London, 2004.
[43] M. Rubinstein, R.H. Colby, A.V. Dobrynin, Physical Review Letters 73 (1994) 2776.
[44] E. Mitsoulis, Journal of Non-Newtonian Fluid Mechanics 74 (1998) 263.
[45] R.P. Chhabra, Bubbles, drops, and particles in non-Newtonian fluids. 2nd ed., CRC Taylor & Francis, Boca Raton, FL, 2007.
[46] R. Clift, J.R. Grace, M.E. Weber, Bubbles, drops, and particles. Academic Press, New York, 1978.
[47] I. Machač, B. Šiška, L. Machačová, Chemical Engineering and Processing: Process Intensification 39 (2000) 365.
[48] Z. Yu, A. Wachs, Y. Peysson, Journal of Non-Newtonian Fluid Mechanics 136 (2006) 126.
[49] E. Allen, P.H.T. Uhlherr, Journal of Rheology 33 (1989) 627.
[50] S. Daugan, L. Talini, B. Herzhaft, Y. Peysson, C. Allain, Oil and Gas Science and Technology 59 (2004) 71.
[51] G. Gheissary, B.H.A.A. van den Brule, Journal of Non-Newtonian Fluid Mechanics 67 (1996) 1.
[52] S. Daugan, L. Talini, B. Herzhaft, C. Allain, The European Physical Journal E: Soft Matter and Biological Physics 7 (2002) 73.
[53] S. Mahammad, R.K. Prud'homme, G.W. Roberts, S.A. Khan, Biomacromolecules 7 (2006) 2583.
[54] M.D. Burke, S.A. Khan, Biomacromolecules 1 (2000) 688.
[55] A. Tayal, R.M. Kelly, S.A. Khan, Macromolecules 32 (1999) 294.
[56] Y. Cheng, R.K. Prud'homme, Biomacromolecules 1 (2000) 782.
[57] M.A. Rao, Rheology of Fluid and Semisolid Foods - Principles and Applications. Springer - Verlag, 2007.
[58] P.B. Welzel, S. Prokoph, A. Zieris, M. Grimmer, S. Zschoche, U. Freudenberg, C. Werner, Polymers 3 (2011) 602.
[59] Z.H. Guo, Z.P. Fang, Chinese Journal of Polymer Science (English Edition) 27 (2009) 183.
[60] H.H. Winter, M. Mours, in: (Ed.)^(Eds.), 1997, p 164.
[61] W.P. Cox, E.H. Merz, Journal of Polymer Science 28 (1958) 619.
[62] T. Tosco, D.L. Marchisio, F. Lince, R. Sethi, Transport in Porous Media 96 (2013) 1.

Figures

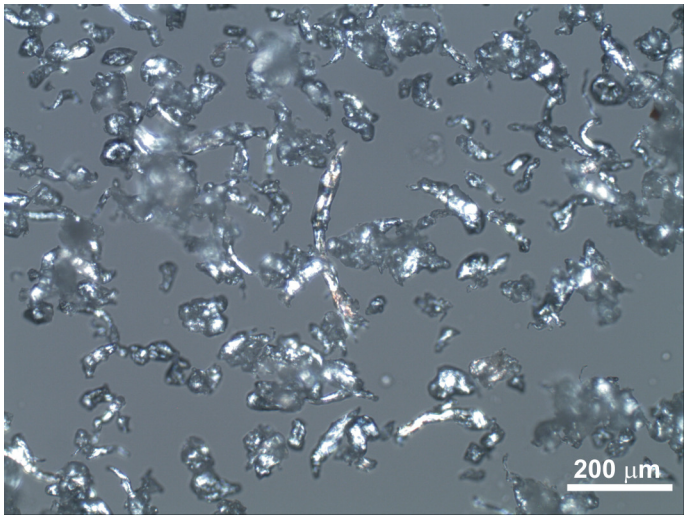

Figure 1: Optical microscope images of guar gum dry powder (RANTEC HV7000).

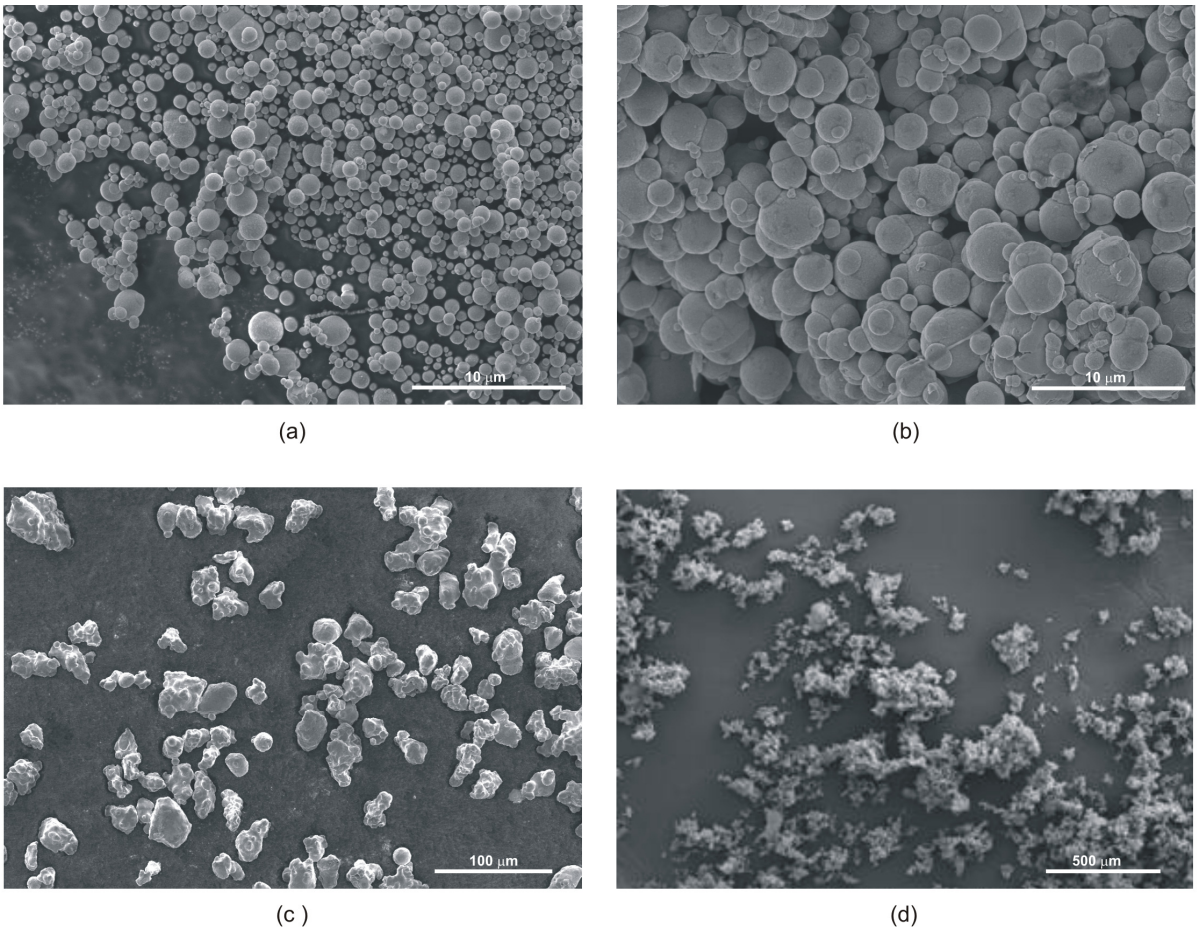

Figure 2: SEM images of iron microparticles: (a) BASF HQ, (b) BASF MS200, (c) Höganäs H4 and (d) Höganäs H19.

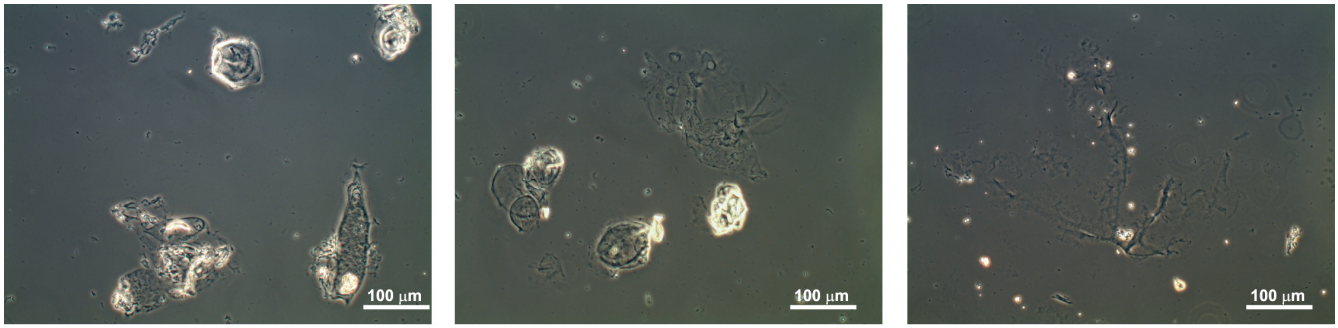

(a) (b) (c)

Figure 3: Optical microscope images of guar gum solutions prepared with procedure AR (a), T60 (b) and T60C (c).

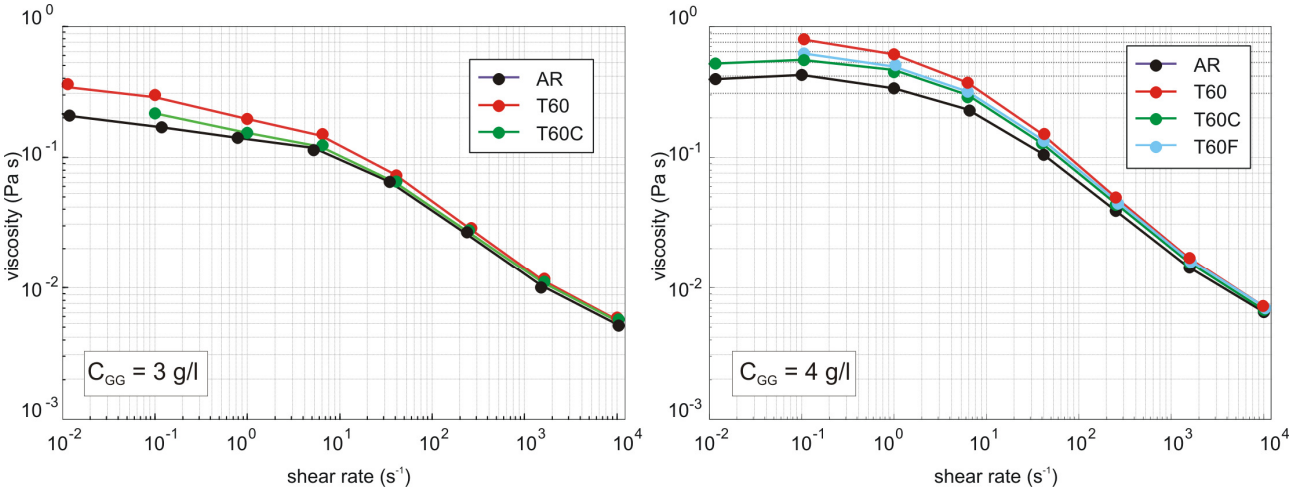

(a) (b)

Figure 4: Rheological curves of guar gum solutions at 3 g/l (a) and 4 g/l (b) for several preparation procedures.

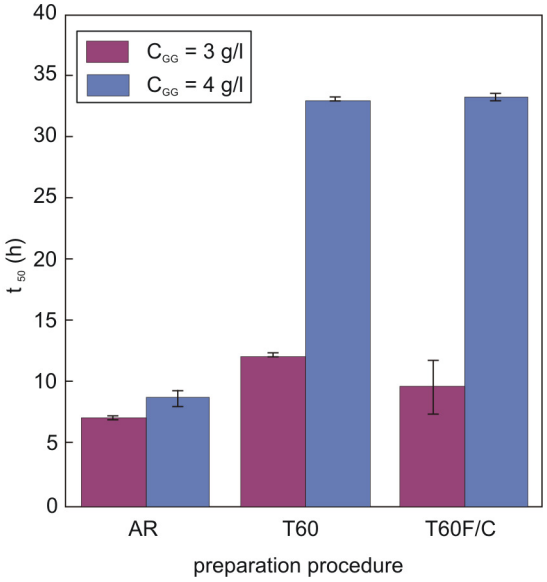

Figure 5: Sedimentation half time of HQ microparticles dispersed in 3 g/l and 4 g/l guar gum solutions, prepared applying different procedures (AR = as received; T60 = dissolved in warm water at 60°C; T60C/F = dissolved in warm water and centrifuged or filtered).

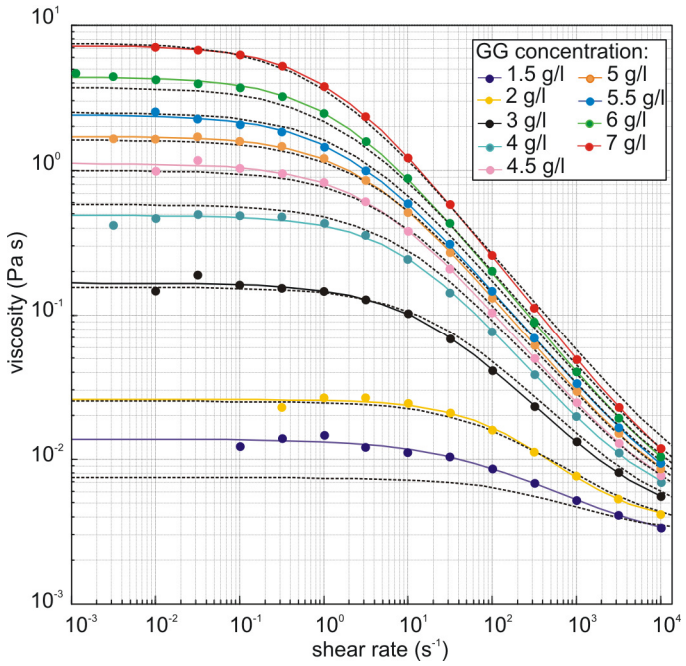

Figure 6: Steady state viscosity of guar gum solutions for concentrations in the range 1.5 to 7 g/l. Points represent the experimental values, solid lines represent the Cross curves fitted separately for each guar gum concentration, dashed lines report the viscosity curves calculated using the model eq. (6).

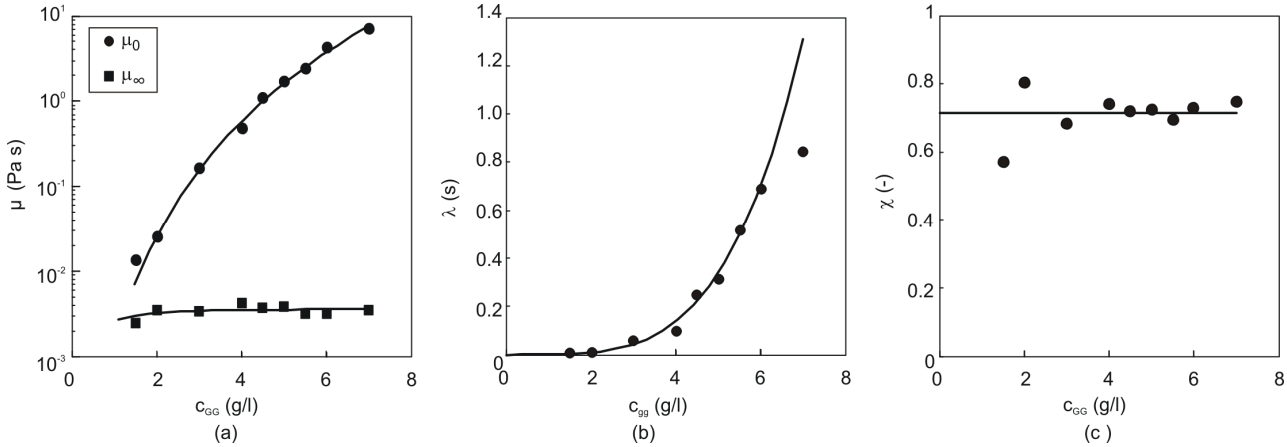

Figure 7: Cross parameters as a function of guar gum concentration. The points correspond to the values obtained from inverse-fitting with the Cross model of each experimental rheogram. The lines represent the inverse-fitted model eq. (8).

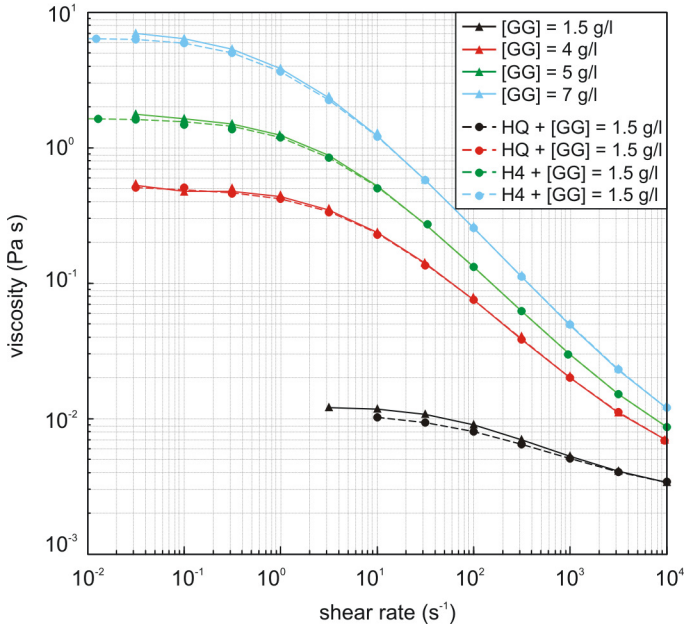

Figure 8: Steady state viscosity of guar gum solutions (1.5, 4, 5, 7 g/l) and dispersions of HQ and H4 particles (20 g/l) in the same guar gum solutions.

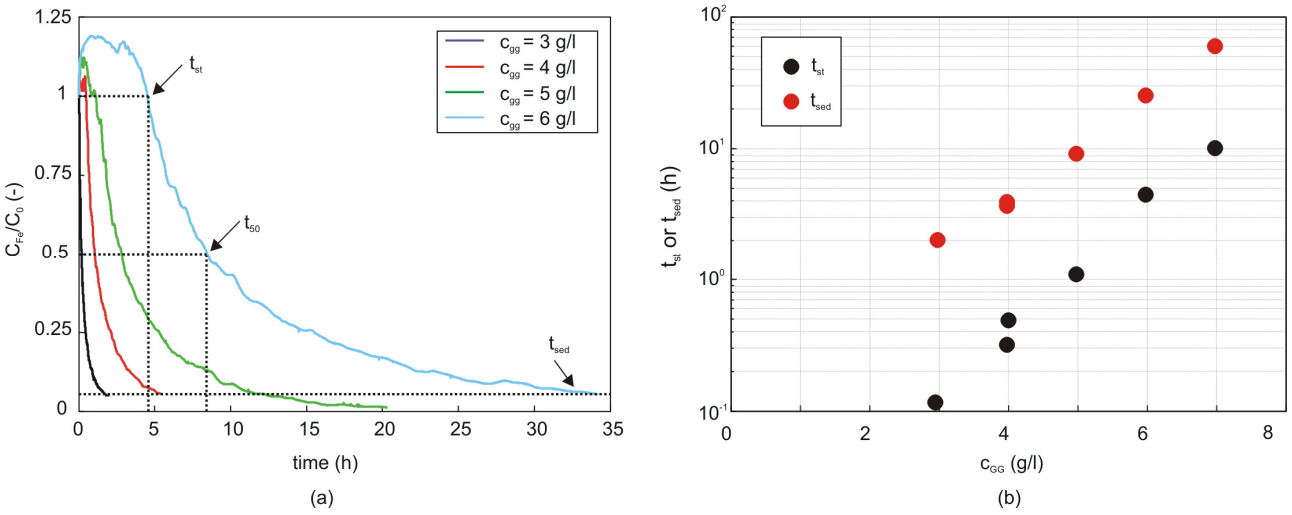

Figure 9: Sedimentation curves for H4 particles dispersed in guar gum (3 to 7 g/l) (a) and characteristic times t_{st} and t_{sed} as a function of guar gum concentration for H4 particles (b).

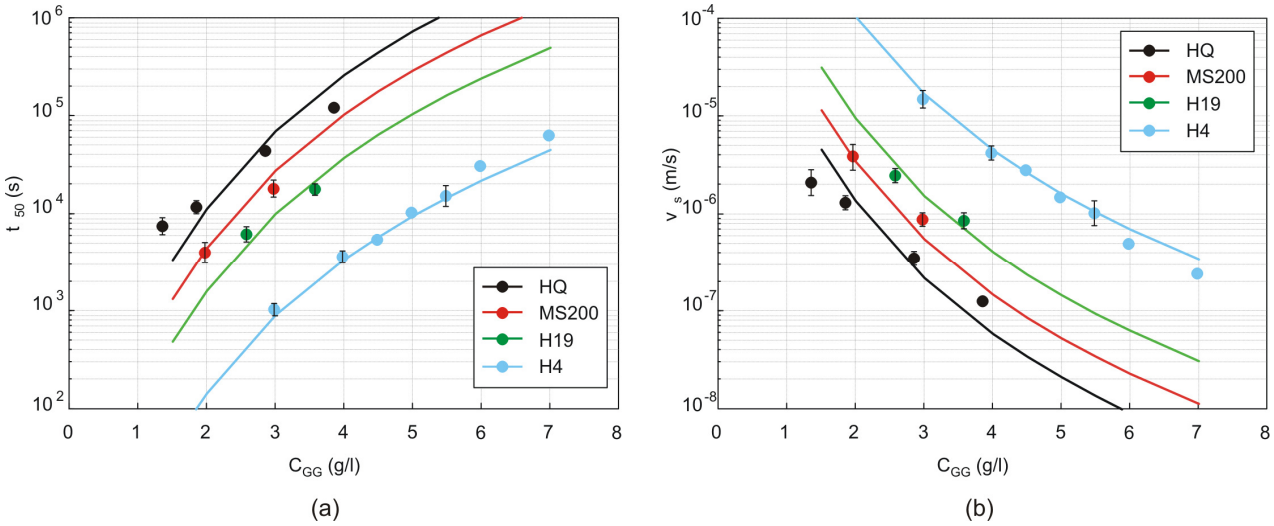

Figure 10: Sedimentation half time t_{50} (a) and corresponding sedimentation rate v_s (b) for HQ, MS200, H19 and H4 particles dispersed in guar gum. The values are determined from sedimentation rates (point values) and estimated from the modified Stokes law (8) (lines).

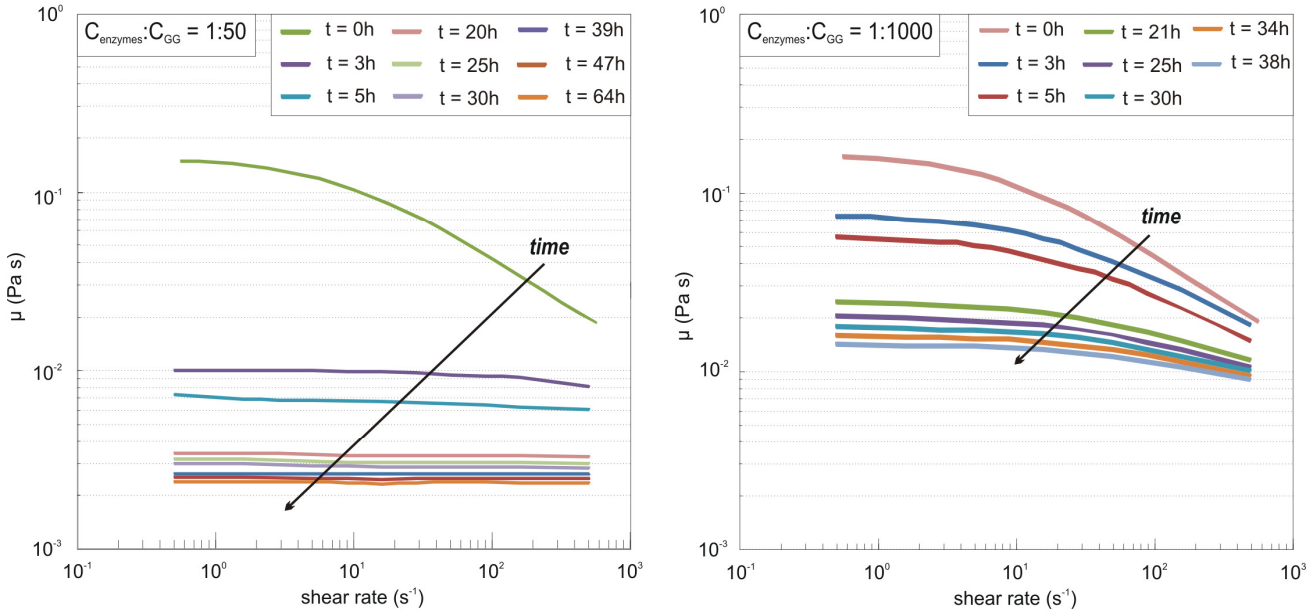

Figure 11: Shear viscosity of 3 g/l guar gum solution as a function of shear rate measured at different times during the degradation process for enzymes concentrations equal to (a) 1:50 and (b) 1:1000.

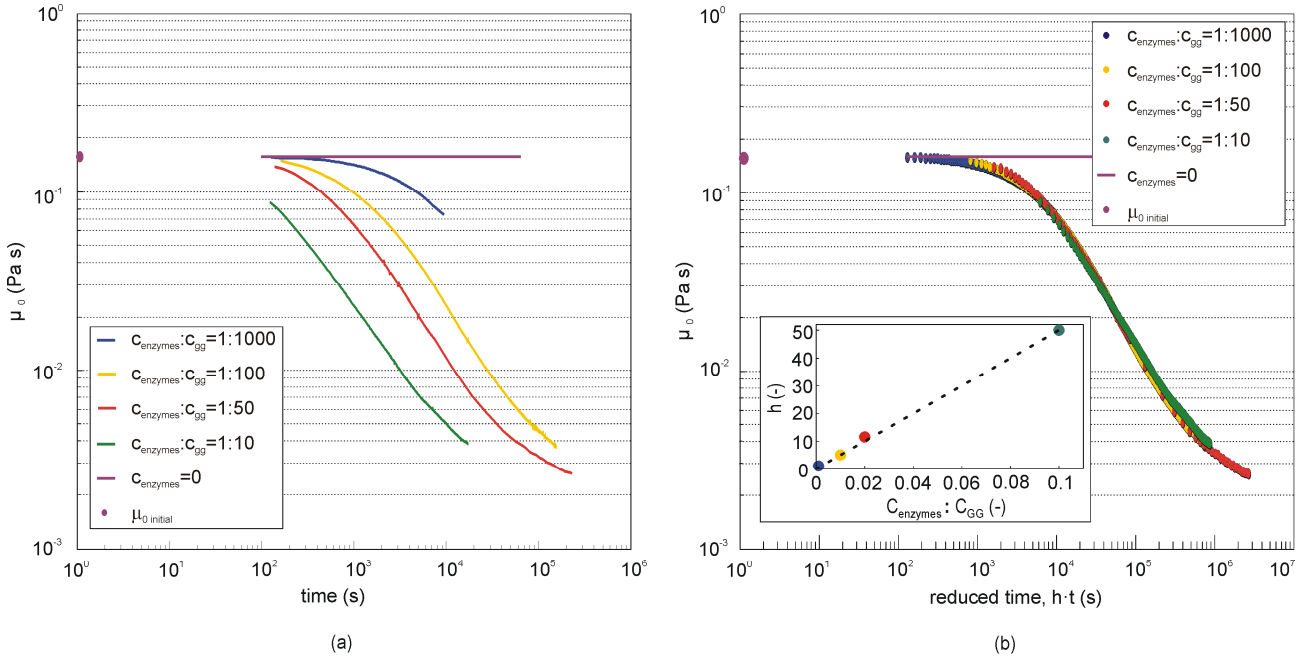

Figure 12: Degradation kinetics of 3 g/l guar gum solution for different enzymes concentrations (1:10, 1:50, 1:100, 1:1000) at a constant frequency (1 rad/s), (b) master curve of viscosity reduction. In the box in (b) the applied shift factor as a function of enzymes concentrations is reported.

Table

Table 1: Particle size distribution, equivalent Stokes diameter and BET.

	Measured d_{50} (µm)	Average eccentricity (-)	Aggregates	$d_{50,Stokes}$ (µm)	B.E.T. (m^2/kg)	Guar gum adsorbed (g/l)
BASF HQ	1.2	0	Yes	1.9 (+)	855 (*)	0.15
BASF MS200	4.7	0	No	4.7 (++)	218.2 (*)	0.03
H4	28.7	0.5	No	22.7 (++)	94 (**)	0.16
H19	8.0	0.24	No, spongy structure of primary particles	7.8 (++)	2397 (**)	0.42
(+) average equivalent diameter of the sphere with same volume as the aggregate; (++) average equivalent diameter of the sphere with same volume as primary particle, obtained from SEM image analysis; (*) estimated as sphere surface to sphere mass; (**) value provided by the producer						